DTIP 2-4 April 2014, Cannes Côte d'Azur, France

Characterization of Capacitive Micromachined Ultrasonic Transducers

Joseph Lardiès, Fayçal Bellared, Brahim Belgacem, Gilles Bourbon, Patrice Le Moal, Vincent Walter
Institute FEMTO-ST; DMA; UMR CNRS 6174
24, Rue de l'Epitaphe
25000 Besançon, FRANCE

***Abstract* — This communication describes numerical and experimental characterization of CMUTs for ultrasound transmission. Simulations based on finite elements method to model CMUTs electromechanical behaviour and to determine the dimensions of elementary cells are presented. In particular we analyze the collapse voltage variations for different parameters of a circular cell and the capacitance variations for different bias voltages. We report the deformations of non-metallized and metallized membranes and we determine eigenfrequencies, bandwidth and quality factors of cells. The fabrication of CMUTs is based on the anodic bonding of a SOI wafer on a borosilicate glass substrate and we compare experimental results with numerical results.**

Keywords- CMUTs, collapse voltage, fill factors, capacitance variations

I. INTRODUCTION

Capacitive Micromachined Ultrasonic Transducers (CMUTs) are MEMS based structures that can be used to generate and sense acoustic signals in the ultrasonic range. CMUTs are constituted by a very large number of membranes and constitute a competitive instrument for ultrasound arrays used in medical imaging and non destructive testing. CMUTs offer advantages, in comparison with piezoelectric sensors, due to their small size, high sensibility, wide bandwidth, wide directivity, improved image resolution, batch fabrication capability, ease of integration with CMOS and low power consumption. The basic element of a CMUT is a capacitor that is a structure comprising two electrodes facing each other, one of which is fixed: a back plate and the other is movable: a flexible membrane that can be metallized and can vibrate. The two electrodes are separated by an insulating layer and an air gap. If an alternating voltage, applied between the membrane and the back plate, is superimposed on the bias voltage the modulation of the electrostatic force results in membrane vibrations with generation of ultrasonic waves. The idea of generating acoustic waves by the electrostatic attraction force between the plates of a capacitor is very old and a tutorial can be obtained in [1]. A good design of a capacitive sensor requires a large displacement of the membrane and optimum energy coupling between the membrane and the air is achieved when the membrane is near the structural instability known as pull-in [2-5]. The largest stable membrane deflection occurs for the pull-in voltage or collapse voltage. Beyond this point, the movable membrane snaps onto the fixed plate (or substrate). Many resonance applications demand better understanding of a cell behavior, especially near the pull-in instability, and finite element method (FEM) simulations and analytical plate or membrane models have been used to analyze resonance microstructures effects [4, 5].

Several parameters contribute to the evaluation of the final performance of a CMUT: membrane thickness, membrane radius, electrode thickness, collapse voltage, metallization fill factor, gap height, and mechanical properties of the CMUT such as flexural rigidity, density and relative permittivity. The effectiveness of a CMUT is analyzed in terms of collapse voltage, first resonant frequency, bandwidth sensitivity, electromechanical coupling, electrical impedance and capacitance variations. Different modeling approaches can be found in the literature from the most simple 1D mass-spring analysis [4] up to a large scale computing using finite element models for the calculation of electrical and mechanical fields including the acoustic pressure radiation [3,5].

CMUTs consist of an array of non-metallized or metallized micro-membranes suspended over a substrate. CMUTs are commonly fabricated by means of the surface micromachining technology, using standard integrated circuits techniques. Several processes have been reported in the literature to fabricate CMUTs, using different materials and thin-film deposition techniques; integrations with CMOS electronics have been also presented. In our experimental test the CMUTs have been fabricated using the anodic bonding technology [5, 6]. The bonding technology is a particularly promising technique for CMUTs fabrication because it is easy and reliable to control and reduces process cost and time. It does not require a chemical process and a post heat treatment at high temperatures. In comparison with fusion bonding, the surface quality requirement of anodic bonding is much tolerant and does not require an ultraclean environment. Other advantages are benefits of electrical, thermal and optical properties of the glass which is resistant to many chemicals and can be microstructured and joined to many metals. It provides dielectric isolation that significantly reduces parasitic capacitance. This technology enables fabrication of large membranes with large gaps, and can expand the frequency span of CMUTs to a low frequency operation range. Moreover,

 ISBN:

anodic-bonding-based CMUT technology provides design flexibility in terms of choice of materials and fabrication of membranes with different thickness profiles. In this communication, we fist present simulations based on finite elements method, with the help of COMSOL 3.5a FEM software, to model the CMUTs electromechanical behaviour and to determine the dimensions of elementary cells and networks. Static and dynamic analyses are performed to observe the electromechanical comportment of membranes. Thereafter we analyze the experimental results obtained from CMUTs which have been realized using the anodic bonding technology.

II. NUMERICAL ANALYSIS OF CMUTS

A. *Modelization of a capacitive cell*

The cells use a monocrystalline silicon membrane suspended over a metallic electrode deposited at the bottom of a cavity defined into a glass wafer. To simplify the design, no isolation layer between the membrane and the bottom electrode is considered and the cavities are assumed vacuum sealed. The cells are designed for working under a maximum bias voltage of 200 V and in a frequency range from 100 kHz to 5 MHz. We perform the design of CMUT cells with the help of the COMSOL 3.5a FEM software. An effort is made to build simplified models, which are nevertheless able to accurately simulate various aspects of CMUT operating mode. Static and dynamic analyses are conducted to provide an in-depth understanding of device behaviour and coupling mechanisms. All analyses are performed for a circular silicon membrane clamped at its edges and covered with a centred circular aluminium top electrode. An example of a simulated CMUT cell is shown in Fig.1.

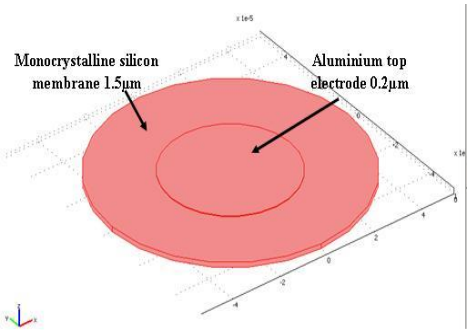

Fig. 1. COMSOL model for a circular CMUT.

Table 1 summarizes the geometrical and physical properties of the modeled CMUT structure. It is assumed that all materials are isotropic.

TABLE 1
GEOMETRIC AND PHYSICAL PROPERTIES OF THE CMUT

Function	Material	Thickness [µm]	Young modulus (GPa)	Poisson ratio	Density (kg/m^3)	Relative permittivity
Top electrode	Aluminium	0.1 - 0.4	70	0.35	2700	-
Membrane	Silicon	1.5 - 2	131	0.27	2330	11.7

B. *Static analysis and collapse voltage estimation*

The static analysis allows the determination of CMUT cells radius and the best metallization fill factor FF defined as the ratio of top electrode radius to the membrane radius [5]. The membrane deformation due to the applied bias voltage is used to find collapse voltage and device capacitance. The model simulates the electromechanical interaction through the application of an electrostatic force which is dependent on the transverse deformation. Using COMSOL, the CMUT collapse voltage is found iteratively where the applied voltage is increased at each step, and the convergence is verified to obtain the solution. The static solution resulting at one third gap height displacement is taken as the collapse voltage. We performed series of parametric static analysis on different membrane radius (from 20µm to 150µm) and Fill Factors (from 50% to 100%). Fig.2 shows the collapse voltage variation as a function of membrane radius for both a non-metallized (FF=0%) and a metallized membrane with different FF factors. In this example the top electrode thickness te is equal to 0.2 µm. For FF=0%, the membrane is composed of a heavily doped silicon without a metallization layer.

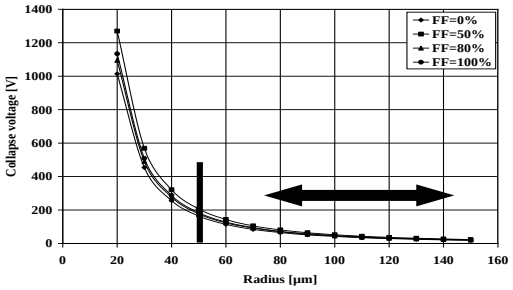

Fig. 2. Collapse voltage as a function of membrane radius.

From Fig.2 the collapse voltage decreases with increasing membrane radius for all FF values. If an actuation voltage limit of 200 V is considered as the maximum working point, the smallest cell radius satisfying this voltage is R = 50 µm.

We consider now four membranes of radius : 50 µm, 70 µm, 100 µm and 150 µm. Fig. 3 shows the collapse voltage variations as a function of FF for different membrane radius. A higher voltage is necessary for the collapse of a membrane with a smaller top electrode.

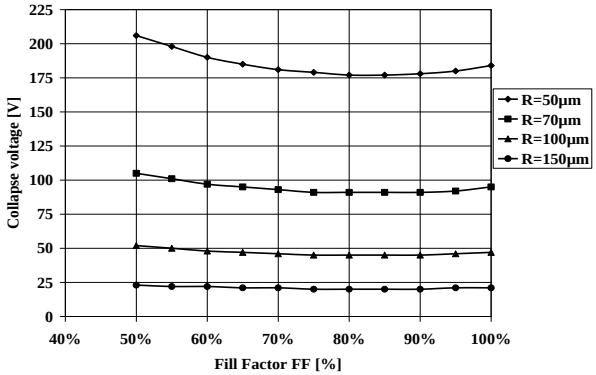

Fig. 3. Collapse voltage as a function of fill factor for different membranes.

From Fig. 3 it is shown that a FF of 80% is found to give the lowest collapse voltage for each membrane radius. For FF values smaller than 80% the electrostatic force is inferior to the membrane stiffness force and the resulting displacement of the membrane is smaller. Higher voltages are then necessary to bring the cell to collapse. For FF values higher than 80% the deflections of the membrane are also smaller and collapse voltages are higher.

Table 2 summarizes the estimated collapse voltages for different membranes radius and fill factors.

TABLE 2
ESTIMATED COLLAPSE VOLTAGES

Radius (µm)	FF=0% Collapse voltage [V]	FF=80% Collapse voltage [V]
50	164	177
70	84	92
100	42	45
150	19	20

Fig. 4 presents the influence of gap height tg for different values of the top electrode thickness te on the collapse voltage for both : a non-metallized membrane with R = 50 µm, FF = 0%, and te = 0 µm and a metallized membrane with R = 50 µm and FF = 80% .

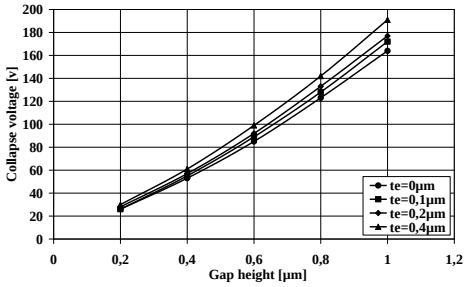

Fig. 4. Collapse voltage variations as function of gap height for different top electrode thickness.

Decreasing the gap height and the top electrode thickness reduces the collapse voltage significantly. A thin electrode is advantageous in terms of reducing the metal/membrane bilayer rigidity. However from a technical point of view, we decide to use a top electrode thickness of 200 nm to obtain sufficient electrical conductivity. Table 3 summarizes the CMUT cells dimensions used in this study which are derived from collapse voltage computations. The effective gap thickness considered will be 1 µm.

TABLE 3
CMUT CELL DIMENSIONS

	Material	Radius (µm)				Thickness (µm)
Membrane	Silicon	50	70	100	150	1.5
Electrodes	Gold/Aluminium	40	56	80	120	0.2

C. *Eigenfrequencies of membranes estimation*

A 3D eigenfrequencies analysis is performed on CMUT structures for different membrane radius. Fig. 5 shows the plot of the two first vibration modes for a cell with R=50 µm and FF=0%.

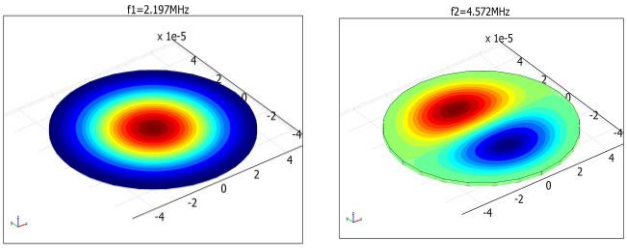

Fig. 5. Two first vibration modes of the membrane.

Table 4 gives the first eigenfrency of the structures used in this study. The resonance frequency decreases as the membrane radius increases and has the same behavior for FF=0% and FF=80%.

TABLE 4
EIGENFREQUENCIES OF CMUT CELLS

	FF=0%				FF=80%			
R (µm)	50	70	100	150	50	70	100	150
f (MHz)	2.19	1.12	0.55	0.24	2.18	1.11	0.54	0.24

D. *Capacitance estimation*

The static analysis results are used to determine the input capacitance of CMUT cells. The capacitance is estimated by inserting the deflection values w (due to the AC bias) of the silicon membrane surface for a non-metallized membrane or the top electrode/membrane interface surface for a metallized membrane in the expression given in (1) [5]. ε_0 is the permittivity of the free space and t_{geff} the effective gap thickness. The integration is computed on the considered surface A. Table 4 summarizes the estimated values of the static capacitance for different membrane radius and for two configurations: FF=0% and FF=80% using COMSOL.

$$C_{FEM} = \int_A \frac{\varepsilon_0 \, ds}{(t_{geff} - w)} \qquad (1)$$

TABLE 5
STATIC CAPACITANCE OF NON-METALLIZED AND METALLIZED MEMBRANE CELLS

C (pF)	R [µm]			
	50	70	100	150
FF=0%	6.16×10^{-2}	1.20×10^{-1}	2.46×10^{-1}	5.54×10^{-1}
FF=80%	3.94×10^{-2}	7.72×10^{-2}	1.57×10^{-1}	3.54×10^{-1}

The capacitance variations as a function of the applied bias voltage are then obtained by using a series of static analyses. Fig.6 shows the capacitance variations for two configurations: FF=0% (a) and FF=80% (b) with R = 50 µm and tm = 1.5 µm.

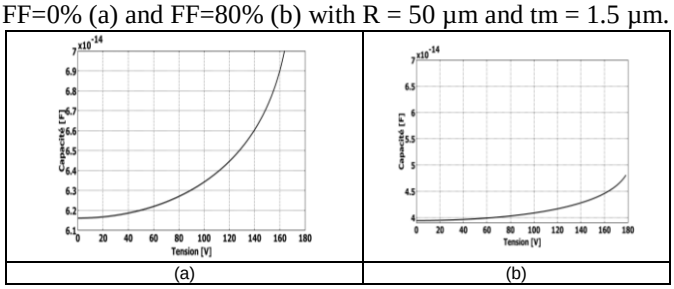

Fig.6. Capacitance variations as a function of the applied voltage.

III. EXPERIMENTAL CMUTs CHARACTERIZATION

A. Experimental static deformation characterization

Fabrication of CMUTs has been performed using anodic bonding of a fixed thickness monocrystalline silicon layer of a SOI wafer on a borosilicate glass substrate [5, 6]. The process evolution for each technological step and the fabrication runs are not discussed in this communication but details can be found in [5]. The residual deformations of CMUT cells were measured for the non-metallized membranes using the MSA500 microsystem analyzer (Polytec) and for the metallized membranes using the Alpha step IQ (Tencor) profilometer. For metallized membranes a FF=80% is used.

For non-metallized membranes, the residual deformation is evaluated by performing two diagonal readings from two perpendicular scans allowing the measurement of vertical and horizontal lines deformations. When these two deformations are identical, the cell is considered uniform. According to the obtained curvature (upwards or downwards), the cell is said to be concave or convex. Fig. 7 shows the experimental residual deformation for a cell of radius R= 100 µm. The cell is uniform, concave and has, at its center, a residual deformation of about 110 nm.

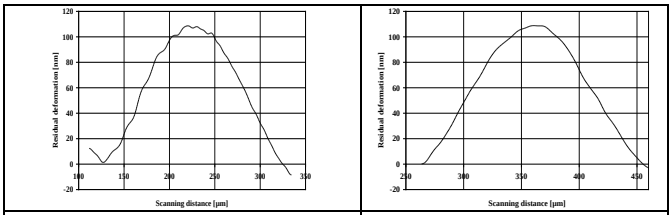

Fig. 7. Measurement of residual deformation of a non-metallized cell in horizontal line (a) and in vertical line (b).

Table 6 shows the measured residual deformations, at the center of the membrane, for different unit cells and network cells with non-metallized membranes. D_{RM} is the mean value of the residual deformation measured for all cells (concave and convex) and σ is the standard deviation.

TABLE 6
RESIDUAL DEFORMATIONS OF NON-METALLIZED MEMBRANES

Radius (µm)			Concave	Convex
50	Unit cell	Cells number	8	0
		Deformation [nm]	(D_{RM}=32, σ=7)	
	Network	Cells number	28	5
		Deformation [nm]	(D_{RM}=23, σ=12)	
70	Unit cell	Cells number	9	3
		Deformation [nm]	(D_{RM}=41, σ=8)	
	Network	Cells number	4	4
		Deformation [nm]	(D_{RM}=54, σ=19)	
100	Unit cell	Cells number	13	2
		Deformation [nm]	(D_{RM}=2069, σ=1337)	
	Network	Cells number	178	15
		Deformation [nm]	(D_{RM}=429, σ=476)	
150	Unit cell	Cells number	32	6
		Deformation [nm]	(D_{RM}=2368, σ=1153)	
	Network	Cells number	91	14
		Deformation [nm]	(D_{RM}=1656, σ=554)	

Deformations values obtained for cells of radius 50 µm, 70 µm are very low and increase as radius increase. We note that the residue becomes very important for 100 µm and 150 µm radius cells.

B. Experimental collapse voltage characterization

The results of collapse voltage measurements are shown in Table 7 and Table 8. In these tables we present the mean collapse voltage V_{CM} for different cell radius and the associated standard deviation σ. The theoretical collapse voltages are also presented for comparison purposes. The thickness of the membrane is t_m = 1.5 µm and the thickness of the gap is t_g = 1µm. The FF is 80% for metallized membranes.

TABLE 7
COLLAPSE VOLTAGE MEASUREMENTS OF NON-METALLIZED MEMBRANES

R (µm)	Theoretical V_{CM} (V)	Number of cells	Experimental V_{CM} (V)	Relative error (%)
50	164	9	V_{CM}=156, σ=28.74	5.13
70	84	8	V_{CM}=88.75, σ=11.37	5.35
100	42	7	V_{CM}=70.28, σ=18.15	40.24
150	19	13	V_{CM}=66.15, σ=11.94	71.28

TABLE 8
COLLAPSE VOLTAGE MEASUREMENTS OF METALLIZED MEMBRANES

R µm	Theoretical V_{CM} (V)	Number of cells	Experimental V_{CM} (V)	Relative error (%)
50	177	5	V_{CM}=180, σ=19.8	1.6
70	92	6	V_{CM}=94.83, σ=6.43	3
100	45	5	V_{CM}=54, σ=11.52	16.67
150	20	5	V_{CM}=34, σ=7.39	41.18

For 50 µm and 70 µm radius membranes the error between theoretical and experimental collapse voltage is very low. For 100 µm and 150 µm radius membranes the error between theoretical and experimental collapse voltage becomes important. Indeed, large cells (R≥100µm) are more constrained and show a higher residual deformation than smaller cells. They require therefore higher polarization voltages to bring them to pull-in. This behaviour is also observed during the frequency response analysis presented in the next section.

C. Experimental eigenfrequencies characterization

Frequency analysis is based on the measurement of the FFT from the step response of CMUT cells. The spectrum is used to obtain the -3dB bandwidth. All cells are excited by an AC voltage of 10 V peak to peak. The average values of the resonance frequency f_{RM}, the bandwidth B, the mechanical quality factor Q_M in the air and the associated standard deviations σ are shown in Table 9 for non-metallized cells and in Table 10 for metallized cells. The theoretical resonance frequencies are shown for comparison purposes. For t_m=1.5 µm, the frequency response is fairly homogeneous (low dispersion around mean value) for all unit cells and networks. For 50 µm and 70 µm radius membranes the error between theoretical and experimental resonance frequencies are between 7% and 17%, which is relatively low. However, this error grows as the radius increases: for 100 µm and 150 µm radius membranes the error between theoretical and experimental resonance frequencies are between: 24% and 60%. The differences are related to the residual deformations due to residual stresses in the CMUTs membranes which are more important for large radius cells. Such tensile or compressive stresses tend respectively to increase or decrease the resonance frequencies of the membranes. In our case, it appears that large radius membranes are under tensile stresses.

TABLE 9
EGENFREQUENCIES , BANDWIDTH AND QUALITY FACTOR OF NON-METALLIZED MEMBRANES

R (µm)	Cells number	Theoretical frequency (MHz)	Experiment. frequency (MHz)	Relative error (%)	B (KHz)	Q_M
Unit cells						
50	46	2.19	(f_{RM}=2.372, σ=0.164)	7.67	(B_M=73.037, σ=14.302)	(Q_M=35.592, σ=9.338)
70	28	1.12	(f_{RM}=1.341, σ=0.252)	16.48	(B_M=98.562, σ=9.943)	(Q_M=12.492, σ=1.103)
100	45	0.55	(f_{RM}=0.759, σ=0.021)	27.53	(B_M=102.291, σ=11.463)	(Q_M=7.594, σ=0.853)
150	63	0.24	(f_{RM}=0.586, σ=0.037)	59.04	(B_M=69.126, σ=6.484)	(Q_M=8.417, σ=0.708)
Networks						
50	6	2.19	(f_{RM}=2.264, σ=0.023)	3.26	(B_M=68.166, σ=13.421)	(Q_M=34.599, σ=7.109)
70	6	1.12	(f_{RM}=1.238, σ=0.071)	9.53	(B_M=133.6, σ=74.37)	(Q_M=11.272, σ=3.872)
100	10	0.55	(f_{RM}=0.759, σ=0.029)	27.53	(B_M=104.122, σ=6.107)	(Q_M=7.402, σ=0.431)
150	22	0.24	(f_{RM}=0.576, σ=0.008)	58.33	(B_M=63.914, σ=4.013)	(Q_M=9.051, σ=0.602)

TABLE 10
EGENFREQUENCIES , BANDWIDTH AND QUALITY FACTOR OF METALLIZED MEMBRANES

t_m=1.5 µm						
R [µm]	Cells number	Theoretical frequency [MHz]	Experiment. frequency [MHz]	Relative error [%]	B [KHz]	Q_M
Unit cells						
50	13	2.17	(f_{RM}=2.333, σ=0.123)	7	(B_M=74.4, σ=0.909)	(Q_M=30.983, σ=1.435)
70	8	1.11	(f_{RM}=1.303, σ=0.053)	14.81	(B_M=96.7, σ=15.062)	(Q_M=13.273, σ=2.04)
100	6	0.54	(f_{RM}=0.836, σ=0.07)	35.41	(B_M=89.993, σ=6.426)	(Q_M=10, σ=0.836)
150	6	0.24	(f_{RM}=0.605, σ=0.013)	60.33	(B_M=60.333, σ=5.583)	(Q_M=10.396, σ=1.064)
Networks						
50	4	2.17	(f_{RM}=2.205, σ=0.203)	1.59	(B_M=91.833, σ=5.216)	(Q_M=22.94, σ=1.357)
70	3	1.11	(f_{RM}=1.26, σ=0.028)	11.9	(B_M=70.566, σ=13.406)	(Q_M=18.523, σ=3.823)
100	2	0.54	(f_{RM}=0.84, σ=0.024)	35.71	(B_M=85.15, σ=1.51)	(Q_M=9.63, σ=0.21)
150	2	0.24	(f_{RM}=0.607, σ=0.009)	60.46	(B_M=58.7, σ=0.697)	(Q_M=10.313, σ=0.231)

The average values of mechanical quality factor Q_M decreases with increasing membrane radius and exhibit a variation which is proportional to the square of the ratio "membrane thickness/membrane radius" ($Q_M \sim (t_m/R)^2$)]. The quality factor, and therefore the dissipation level, depends on the size of the CMUT cell and increases with the increase of the square of the ratio t_m/R. The use of a thick membrane and a small cell radius allows optimization of mechanical quality factor. The results of the frequency analysis confirm the collapse voltage measurement.

D. Experimental capacitance characterization

The capacitance variations under bias voltage are derived from impedance measurements. The static capacitance C_0 corresponds to the capacitance at zero bias voltage. The thickness of the membrane is t_m=1.5µm. Table11 shows the experimental results for different radius of cells.

TABLE 11
CAPACITANCE VALUES OF NON-METALLIZED AND METALLIZED MEMBRANE CELLS

	Non-metallized membranes			Metallized membranes			
R	Theoretical C_0 (pF)	Experimental C_0 (pF)	Error [%]	Theoretical C_0 (pF)	Experimental C_0 (pF)	Error [%]	
50	$6.16x10^{-2}$	$5.58x10^{-2}$	10.39	$3.94x10^{-2}$	$4.02x10^{-2}$	2	
70	$1.20x10^{-1}$	$6.49x10^{-2}$	84.9	$7.72x10^{-2}$	$7.47x10^{-2}$	3.35	
100	$2.46x10^{-1}$	$6.25x10^{-2}$	293	$1.57x10^{-2}$	$7.20x10^{-2}$	116.55	
150	$5.54x10^{-1}$	$6.38x10^{-2}$	285	$3.54x10^{-1}$	$1.35x10^{-1}$	162.22	

For non-metallized membranes of 50 µm radius, the measured static capacitance approaches the theoretical value. However, the difference increases rapidly and becomes very important with increasing cell radius. For metallized membranes, the static capacitance for small radius cells (50µm, 70µm) shows a small difference with respect to the theoretical values. The difference is important for large radius cells (100µm, 150µm). By comparison of the results, we deduce that when a metal electrode is deposited over the silicon membrane, the electromechanical performance of the CMUT is improved. Large radius cells show higher residual deformations than small cells which result in lower capacity values.

Fig.8 shows the theoretical and experimental capacitance variations as a function of applied voltage for two metallized CMUT cells with t_m=1.5µm and radius values of 50µm and 150µm.

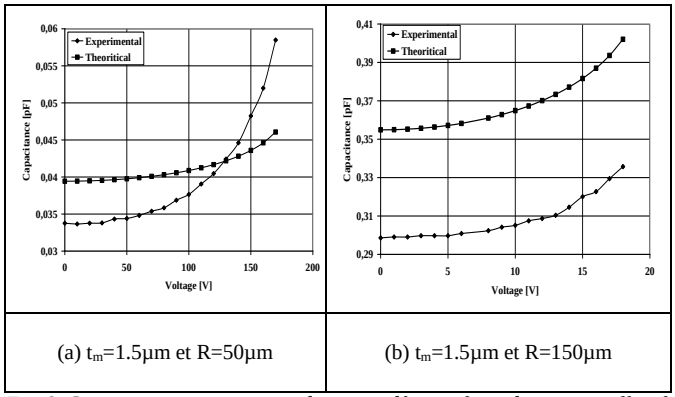

(a) t_m=1.5µm et R=50µm (b) t_m=1.5µm et R=150µm

Fig. 8. Capacitance variations as a function of bias voltage for two metallized CMUT cells.

For the 50µm radius cell experimental results are very similar to theoretical values until a collapse tension of 150 V. For the 150µm cell the experimental values of the capacitance have a constant difference of 0,6 pF with the theoretical values.

E. Electromechanical coupling coefficient

The electromechanical coupling coefficient k_e^2 is evaluated from anti-resonant and resonant frequencies deduced from input impedance and admittance which have been previously measured [5].The electromechanical coefficient is given by [7] :

$$k_e^2 = 1 - \left(\frac{F_r}{F_a}\right)^2 \qquad (2)$$

F_r is the resonant frequency and F_a the anti-resonant frequency. Fig. 9 shows the electromechanical coupling coefficient variations as a function of bias voltage for a metallized CMUT cell. The radius of the membrane is R=50µm, its thickness is t_m=1.5µm and FF = 80%.

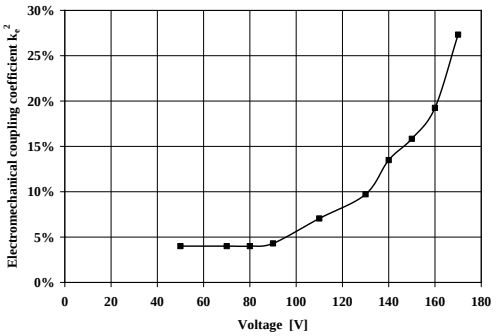

Fig.9. Electromechanical coupling coefficient variations measured for a metallized unit cell.

The electromechanical coupling coefficient changes non-linearly with bias voltage and increases significantly when approaching collapse voltage. At a bias voltage of 170V, we obtain a coupling coefficient of 27%.

IV. CONCLUSION

CMUTs operating in air have been fabricated based on the anodic bonding of a SOI wafer on a borosilicate glass substrate. The results of the models analyzed by FEM have been compared with those obtained experimentally. Mechanical and electrical characterizations have been performed in terms of collapse voltage, eigenfrequencies, bandwidth, quality factor, capacitance and electromechanical coupling. Non-metallized and metallized membranes with the metallized fill factor have been studied and results compared. It is shown that when a metal electrode is deposited over the silicon membrane, the electromechanical performance of the CMUT transducer is improved.

REFERENCES

[1] F.V. Hunt, The Analysis of Transduction and its Historical Back-ground, Harvard University Press, 1982.

[2] A. Caronti, G. Caliano, R. Carotenuto, A. Savoia, M. Pappalardo, E. Cianci and V. Foglietti, '' Capacitive micromachined ultrasonic transducer (CMUT) arrays for medical imaging'', Microelectronics Journal, vol. 37, pp. 770-777, 2006.

[3] C. Meynier, F. Teston and D. Certon, ''A multiscale model for array of capacitive micromachined ultrasonic transducers'', J. Acoust. Soc. Am., vol. 128, pp. 2549-2561, 2010.

[4] J. Lardiès and M. Berthillier, ''A methodology for the pull-in voltage of clamped diaphragms'', DTIP , Aix-en-Provence, 11-13 May 2011.

[5] M.L.F. Bellaredj, ''Méthodes et outils pour la fabrication de transducteurs ultrasonores en silicium'', PhD Thesis, University of Franche-Comté ; July 2013.

[6] W.B.Choi, B.K.Ju Y.H.Lee, "Anodic bonding technique under low temperature and low voltage using evaporated glass," J. Vac. Sci. Technol. , vol. 15(2), Mar/Apr 1997.

[7] G.G.Yaralioglu, A.S.Ergun,B.Bayram,E.Hæggstrom, and BT.Khuri-Yakub, " Calculation and measurement of electromechanical coupling coefficient of capacitive micromachined ultrasonic transducers," IEEE Trans. on Ultrasonics, Ferroelectrics, and Frequency Control, vol. 50, no. 4, April 2003.

 ISBN: